04 Apr 1995, 2:30 pm - 3:30 pm

Efficiency of an Energy-Dissipating Barrier

M. P. Luong
Ecole Polytechnique, Palaiseau, France

Proceedings: Third International Conference on Recent Advances in Geotechnical Earthquake Engineering and Soil Dynamics, April 2–7, 1995, Volume I, St. Louis, Missouri

Efficiency of an Energy-Dissipating Barrier

Paper No. 2.01

M.P. Luong
CNRS-LMS, Ecole Polytechnique, Palaiseau, France

SYNOPSIS The proposed paper describes some experimental procedures, used in (a) laboratory to recognize the energy-dissipating ability of soil and (b) in centrifuge to generate in-flight stress waves propagating through a centrifugal soil mass in order to investigate the efficiency of a stress wave mitigation barrier. The screening principle of this new type of energy-dissipating barrier has been suggested by the dissipative behavior of sandy soils, evidenced by infrared vibrothermography.

INTRODUCTION

A problem of practical importance for the foundation engineer in urban areas is the protection of structures against ground-transmitted waves generated by earthquake hazards and other vibrations such as external traffic, machinery, blasting, which result in ground amplitudes, causing disturbances to adjacent structures. Most of the vibratory energy affecting structures nearby is carried by surface waves that travel in a zone close to the ground surface. The soil may act as a vibration transmitter, thereby modifying the intensity, frequency content and spatial distribution of ground shaking and therefore the structural damage. It is then possible to reduce the ground-borne vibrations significantly by placing a suitable wave barrier in the ground around the structure. The usefullness of such wave barriers is directly associated with the proper isolation of the Rayleigh wave energy. Traditionally, ground vibration isolation, based on the principles of scattering and diffraction of elastic Rayleigh waves, uses rows of cylindrical obstacles installed in the ground, concrete barriers or open and in-filled trenches.

When considering structural isolation, the fundamental rule is that the source of vibration should be dealt with wherever possible, since it is easier to provide anti-vibration mountings for machinery and plant than it is to provide these mountings for buildings. Structural isolation should be considered only in those cases where the external source of vibration cannot be readily controlled or when there still remains an objectionable level of vibration after the source has been treated. Among many suggestions that have been made from time to time to reduce structural vibrations are : (a) the provision of trenches around the building, (b) the use of sand and gravel under the foundations, (c) the choice of most suitable building materials and types of construction, (d) the insertion of diverse especial anti-vibration pads under beam supports and column bases, (e) mounting the complete building, or particular parts of it, on a suitable spring system.

It has been suggested that the presence of a trench or ditch between the source of vibration and the building should reduce transmission of vibration. Many examples of this treatment have been proposed, the majority, however, being unsuccessful. It is extremely doubtful whether the method is suitable for general application, particularly if the vibrations are deep seated (e.g. from drop stamps). Although cases of success have been given, the consensus of opinion is that the method is of little value, unless the trenches are of sufficient depth and are kept open. Barkan (1962) discusses the possible use of trenches and is of the opinion that the depth of a trench should be at least one-third of the wavelength of the vibration. Thus, if the velocity of the vibration in a particular soil were 400 ms^{-1} and the frequency of vibration were 20 Hz, the wave length would be 20 m and the trench would have to be at least 7 m deep. Trenches are therefore likely to be less useful in dealing with low-frequency vibrations (Dolling 1966).

The usefullness of such wave barriers is directly associated with the proper isolation of the Rayleigh wave energy. Traditionally, ground vibration isolation, based on the principles of scattering and diffraction of elastic Rayleigh waves, uses rows of cylindrical obstacles installed in the ground, concrete barriers or open and in-filled trenches. The vibration transmitting properties of various soils have confirmed that each particular type of soil has its own natural frequency, although the expression "site frequency" may be preferable since the resonant frequency will depend on the type of soil and its loading. Since the ground frequency at the surface may differ from that measured at some depth, it is advisable to determine the value at appropriate depth for deep foundations. It cannot be categorically stated that one type of soil is better than another under all conditions, so far its vibration transmission properties are concerned, since both the elasticity and the damping qualities of the soil should be considered. For example, where traffic vibrations have been investigated, lower accelerations have been recorded in sandy soils than in wet clay, whereas vibration has been found to decrease more quickly in wet clay than in sand.

In seismic zones, foundations of civil engineering structures must be designed to resist the effects of strong earthquakes and to undergo substantial deformations without suffering excessive damage or loss of strength in face of subsequent loadings. The major features of seismic wave propagation which have been observed experimentally would be expected on the basis of a purely elastic earth. The pattern of reflected and refracted body waves and the dispersion of surface waves can all be derived by

application of the equations of elasticity to media whose boundaries are chosen to conform to the section of earth involved. However there are differences between observation and theoretical expectation, the principal one being a loss of amplitude in excess of that due to geometrical spreading and reflection at boundaries. How to characterize this decrease of amplitude usually called attenuation, or damping susceptibility of soil foundation against earthquake or dynamic loadings ? The conventional method aims to determine the G shear modulus and the D damping ratio of the soil. The conventional method aims to determine the G shear modulus and the D damping ratio of the soil (Tonouchi et al 1983, Hoar and Stokoe 1984, Mok et al 1988, Ray and Woods 1988, Stewart and Campanella 1991, Teachavorasinskun et al 1991).

In this work, a dimensionless parameter EDI (energy-dissipating index), readily obtained from conventional triaxial test on soil specimen, has been used in order to characterize the stress-strain curve and to express the overall or global dissipativity of soils (Luong 1992). This coefficient permits to quantitatively recognize their energy-dissipating ability. Earthquake damage to structures is often caused by large, permanent deformations of the soil. In all types of soils, these deformations are mostly due to shear failure. In noncohesive soils they can be associated with compaction. In saturated noncohesive soils under certain drainage conditions, there is also the possibility of loss of strength through cyclic mobility or liquefaction. In the laboratory conventional triaxial test, when subjected to several cycles of high-load reversals, this EDI index identifies the nonlinear ductile hysteretic response of soil.

CHARACTERISTIC THRESHOLD

Ground motion studies have been considerably developed, in recent years, using constitutive laws for soils under dynamic, vibratory, cyclic and transient loading. Rheological properties of granular soils have been interpreted at the grain level where the solid particles interact with one another leading to a global aggregation (contractancy) or disaggregation (dilatancy) according to the following main deformation mechanisms : (1) compaction mechanism that forces the solid particles closer together and leads to a denser packing, (2) distortion mechanism governed by irreversible grain slidings dissipating energy by heat, and (3) attrition mechanism caused by breakage of asperities and crushing of grains under high pressures.

Conventional triaxial tests on several sands show that the lowest point on the volume change axial strain curve, that is, the point of minimum volume of the sample, corresponds to a constant stress ratio. The stress peak or maximum of shear resistance occurring at maximum dilatancy rate has been analysed and interpreted by the stress dilatancy theory. The asymptotic part of the stress-strain curve determining the ultimate strength has suggested the well-known critical state concept. For our concern, the transient and cyclic loading cases require the analysis of the prepeak part where the stress ratio η_c at zero dilatancy rate evidently defines the characteristic state of the granular material associated with an angle of aggregate friction ϕ_c (Luong 1980). The characteristic threshold is readily revealed by the appearance of a dilatancy loop when the load cycle crosses the grain interlocking threshold called characteristic state $\eta_c = (q/p)_c$ (zero dilatancy threshold). Using infrared thermography, an experimental approach has evidenced the distortion mechanism occurring in the granular structure and interpreted the main features of the cyclic behavior of sandy soils (Luong 1986).

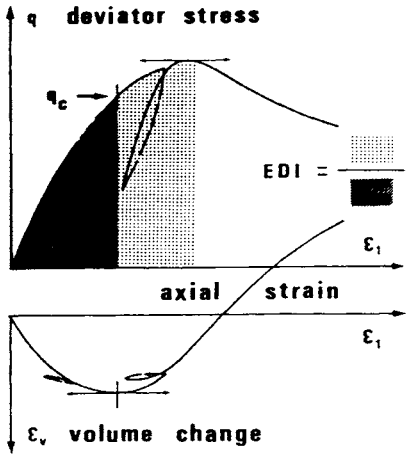

Fig. 1. Definition of EDI energy-dissipating index

Such observations enable the determination of both the entanglement capacity of a granular material and its energy-dissipating ability. Below the characteristic threshold, the intergranular contacts are stable. The limited slidings tend toward a maximal aggregation. In this subcharacteristic domain or contractancy zone, a hysteresis loop occurs when reloading. The mechanical behavior depends on the load history. Above the characteristic threshold, the grain contacts become unstable, leading to significant slidings due to interlocking breakdown. A reload shows a dilatancy loop with memory loss of load history and a softening phenomenon occurs.

Extensive laboratory tests using conventional triaxial apparatus on various sands substantiate these rheological properties. Analysis of experimental curves shows that for a given material, these behaviors do not occur randomly, but they present a continuous evolution with the confining pressure : the dilatancy phenomenon vanishes when the confining pressure increases and prevents the breakdown of granular structure interlocking. The friction angle values ϕ_f and ϕ_c , corresponding respectively to the peak stress and the zero dilatancy stress or characteristic threshold, are calculated according to the Coulomb interpretation for a cohesionless material. The characteristic threshold corresponds in these conditions to the stress threshold where phenomena of disaggregation occur and allow the dissipation of energy generated by relative sliding friction between solid particles.

These experimental observations suggest that, when performing a conventional cylindrical triaxial test, it should be taken into account an energy-dissipating index EDI defined by the ratio of the work W_{dm} mobilized up to the peak strength of the stress-strain curve on the distortional work W_{dc} prior to the characteristic threshold (Fig. 1). Expressed in a dimensionless form, this parameter represents a toughness characteristic of the granular material in a well consistent manner when applied to a wide range of soil behaviors. The larger the EDI index, the better the energy-dissipating ability. The energy-dissipating index may thus be considered as a toughness measure of sandy soil, describing its energy-absorbing ability. In addition, experiments have shown that there occurs no strain-localization in cases of large values of EDI index (>1). Values of EDI index less than 1 correspond to collapsible soils that are highly unstable and dissipate a small amount of energy prior to their catastrophic failure.

ENERGY-DISSIPATING MECHANISM

When a siliceous sand grain slides against another one, there occurs a motion resistance called friction. What is the cause and what really happen on the contact surface ? Bowden and Tabor (1959) demonstrated that when quartz or glass surfaces slide over another in the dark, small sparkling points of light can be seen at the interface. The friction between grains generates heat in the same fashion as when prehistoric man used silex stones to generate fire. With experimental evidence demanding a stress-strain curve independent of strain rate, Coulomb friction immediately suggests itself. For a brick sliding on a flat surface, the horizontal force T is proportional to the normal force N and a coefficient of friction f, $T = fN$. The direction of the force depends on the direction of the relative velocity but not on magnitude of velocity or displacement. If the brick were caused to oscillate, the force-displacement curve would consist of a rectangular hysteresis loop, independent of the frequency of oscillation. For any medium in which seismic waves would cause solid surfaces to slide against each other, the stress-strain diagram should exhibit a closed curve independent of strain rate.

A consideration of the forces and deformations at each contact surface (Mindlin and Deresiewicz 1953) may serve as one starting point in explaining how solid friction affects the force-displacement relations for a sphere pack and in interpreting the thermomechanical coupling of sand behavior under vibratory shearing. For the simplest case of two like spheres, each of radius R, compressed statically by a force N which is directed along their line of centres, normal to their initial common tangent plane, the contact theory caused by Hertz predicts a plane, circular contact radius

$$a = [3 (1 - \nu^2) NR/4 E]^{1/3}$$

where ν and E respectively denotes Poisson's ratio and Young's modulus of the sphere. The normal pressure on the contact area is given by

$$\sigma = 3 N \sqrt{(a^2 - \rho^2)/2 \pi a^3}$$

where ρ represents the radial distance from the centre of the contact circle. An additional tangential force T is assumed to act in the plane of contact, and its magnitude rises monotonically from zero to a given value. Because of symmetry, the distribution of normal pressure remains unchanged. If there is no slip or relative displacement of contiguous points on a portion of the contact surface, the displacement of the contact surface in its plane is constant. The Mindlin's solution of the appropriate boundary-value problem shows that the tangential traction is parallel to the displacement (and to the applied force T) axially symmetric in magnitude, and increases without limit on the bounding curve of the contact area. The key assumption is that on the surface of contact, tangential and normal stresses are governed by Coulomb friction ; that is, at any point where sliding has not occurred, the tangential stress τ must be less than the normal stress multiplied by the friction coefficient $f\sigma$ where f is a constant coefficient of static friction ; and where sliding occurs, the tangential stress equals this value with appropriate sign. In accordance with Coulomb's law of sliding friction, slip is assumed to be initiated at the edge of the contact and to progress radially inward, covering an annular area. The radius c of the adhered portion or the inner radius of the annulus of slip (Fig. 4) is given by

$$c = a (1 - T/f N)^{1/3}.$$

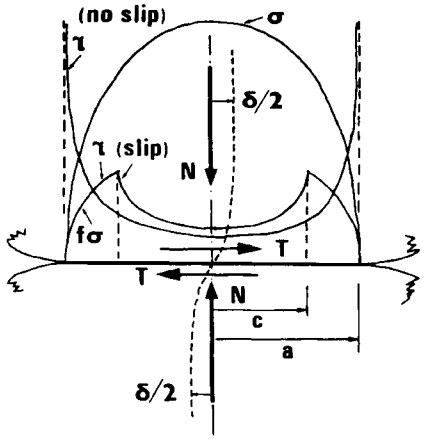

Fig. 2. Stress and strain on contact surface of two like spheres subjected to normal force N followed by a tangential force T

When the tangential force T decreases from a peak value T^*,

$$0 < T^* < f N$$

slip, once again, occurs, but its direction will be opposite to that of the initial slip. An annulus of counter-slip is formed and spreads radially inward as the tangential force is gradually decreased. Its inner radius is

$$b = a [1 - (T^* - T)/2 f N]^{1/3}$$

The inelastic character of the unloading process appears evident since the annulus of the counter-slip does not vanish when the tangential force is completely removed (Fig. 2). Under oscillating tangential forces, the load-displacement curve forms a closed loop traversed during subsequent oscillations of T between the limits $\pm T^*$ providing that the normal force N is maintained constant. The area enclosed in the loop represents the frictional energy dissipated in each cycle of loading. For small tangential forces, it has been suggested that the tangential displacement necessary to relieve the singularity in traction takes the form of an elastic deformation of the asperities. An increase in applied tangential force causes the asperities at the edge of the contact surface to deform plastically through relatively large strains, a process that leads to a marked increase in energy dissipation and to severe damage to the surfaces. Thus at small amplitudes of the tangential force, energy is dissipated as a result of plastic deformation of a small portion of the contact surface, whereas, at large amplitudes, the Coulomb-sliding effect predominates.

In the conventional triaxial test, if the load is cycled within the subcharacteristic domain below the characteristic threshold η_c , the intergranular contacts remain stable. Small slips lead to a maximum entanglement caused by the relative tightening of constituent granules. The dissipated work given by the hysteresis loop "a" in the (deviator stress vs axial strain) plot is relatively small. The corresponding heat production is relatively low and negligible. On the contrary when the shear load is cycled at large amplitude exceeding the characteristic thresholds in triaxial compression and extension, the intergranular contacts become unstable, leading to significant slidings caused by interlocking breakdown. A large frictional energy "B" is dissipated (Fig. 3) and is transformed almost entirely into heat owing to the thermomechanical conversion.

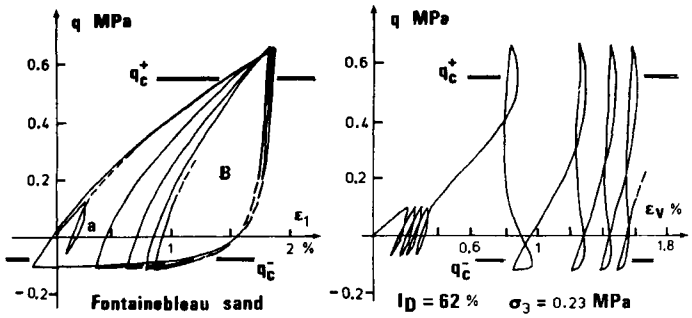

Fig. 3. Conventional triaxial test under small amplitude "a" and large amplitude "B" of deviatoric stress

If the stress peaks in triaxial compression and extension are not exceeded, the resultant effect is densification because the high amplitude loading benefits in partial loss of strain-hardening during the dilating phase in the supercharacteristic domain leading to a breakdown of the granular interlocking assembly. On each reload, the tightening mechanism induces new irreversible volumetric strains and recurs each time with a renewed denser material. This case is particularly interesting when energy needs to be dissipated without risk of soil failure.

THEORETICAL BACKGROUND OF DISSIPATION

The theoretical background of the energy-dissipating mechanism is based on the coupled thermo-visco-elastic-plastic analysis. This leads to a coupled thermomechanical equation where the intrinsic dissipation term is predominant. The work done to the system by plastic deformation is identified as the major contribution to the heat effect. In the framework of thermo-elastic-plasticity, there exists a general acceptance that not all the mechanical work produced by the plastic deformation can be converted to the thermal energy in the solid. A larger portion of the work is believed to have been spent in the change of material microscopic structure. The work done in plastic deformation per unit volume can be evaluated by integrating the material stress-strain curve. This internal dissipation term constitutes an important part of the nonlinear coupled thermomechanical effect. The quantification of this intrinsic dissipation for soils is an extremely difficult task if infrared thermography is not used. This paper emphasizes the advantages of the infrared thermographic technique for the detection of this effect.

Traditionally, the thermomechanical coupling effects have been neglected in thermal analyses. It is generally assumed that the inelastic deformation is rate(time)-independent at low homologous temperatures. The theory of plasticity is consequently formulated in a rate(time)-independent fashion and phenomena such as loading rate sensitivity, creep and relaxation are excluded. The temperature field and the deformation induced by thermal dilation and mechanical loads were solved separately. However this effect could become noticeable if the material is significantly loaded beyond its reversible threshold. The development of the thermo-visco-elastic-plasticity equations requires three types of basic assumptions (Dillon 1963, Kratochvil and Dillon 1969) :

a) The basic thermomechanical quantities describing thermodynamic processes : the motion x, the second Piola-Kirchhoff stress tensor S, the body force per unit mass b, the Helmholtz free energy ψ, the specific entropy s, the heat supply r_0, the absolute temperature T, the heat flux vector per unit area q, the inelastic strain tensor E^I and a set of internal state variables $\alpha^{(I)}$ characterizing the material.

b) The fundamental equations of mechanics postulating for the balance laws of linear momentum, angular momentum, and energy, as well as the second law of thermodynamics expressed in the variables given in a) :

(i) balance of linear momentum

$$\nabla \, SF^T + \rho \, (b - \ddot{x}) = 0 \qquad (1)$$

where F denotes the transformation gradient.

(ii) conservation of energy

$$\rho \, (\dot{\psi} + \dot{s}T + s\dot{T}) = \rho \, \dot{e} = S : \dot{E} - \mathrm{div}\, q + r_0 \qquad (2)$$

(iii) second law of thermodynamics

$$- \rho \, (\dot{\psi} + \dot{s}T) + S : \dot{E} - q . (\nabla T)/T \geq 0 \qquad (3)$$

where ρ is the mass density in the reference configuration ($kg\ m^{-3}$),

e the specific internal energy and

E the Green-Lagrange strain tensor

$E = (\nabla x^T . \nabla x - 1)/2$.

The superposed dot stands for the material time derivative. The continuity equation and the balance of angular momentum are implicitly satisfied in the fundamental equations.

c) The constitutive assumptions describing the material response and abiding the compatibility of the constitutive equations with the fundamental equations of mechanics.

When adopting the separability of the strain tensor

$$E = E^e + E^I + \beta \, (T - T_R) \qquad (4)$$

where β is the coefficient of the thermal expansion matrix, and T_R the reference temperature, the requirement of inequality (4) yields :

(i) The response functions S, ψ and s are independent of the temperature gradient ∇T.

(ii) ψ determines both the stress tensor and the specific entropy through

$$S = \rho \, \partial\psi/\partial E^e \quad \text{and} \quad s = - \partial\psi/\partial T + (\partial\psi/\partial E^e) : \beta$$

(iii) ψ , E^I and q obey the general inequality

$$(S - \rho \, \partial\psi/\partial E^I) : \dot{E}^I - q . \nabla T/T \geq 0 \qquad (5)$$

The above thermodynamic restrictions may now be applied to equation (2) yielding :

$$\rho \, (\partial\psi/\partial E^I - T \, \partial^2\psi/\partial T \partial E^I) : \dot{E}^I - T(\partial S/\partial T) : \dot{E}^e$$
$$- \rho T(\partial^2\psi/\partial T^2)\dot{T} + S : \beta \dot{T} = S : \dot{E}^I - \mathrm{div}\, q + r_0 \qquad (6)$$

Assuming

$$\psi = \psi_0 + (E^e : \overset{4}{D} : E^e)/2 - C_v\, T \ln (T/T_R - 1) \qquad (7)$$

and the Fourier heat conduction law

$$q = - K \operatorname{grad} T \qquad (8)$$

where ψ_0, $\overset{4}{D}$, C_v and K are material constants. $\overset{4}{D}$ stands for the fourth-order elasticity tensor. C_v (J kg^{-1} K^{-1} : Joule per kilogramme per Kelvin degree) is the specific heat at constant deformation and K (W m^{-1} K^{-1} : Watt per metre per Kelvin degree) is the thermal conductivity.

Finally we get the very important following coupled thermomechanical equation :

$$\rho\, C_v\, \dot{T} = K\, \nabla^2 T - (\beta : \overset{4}{D} : \dot{E}^e)\, T + S : \dot{E}^I + r_0 \qquad (9)$$

which shows the varied potential applications and uses of the infrared scanning technique in mechanical engineering. The volumetric heat capacity $C = \rho\, C_v$ of the material is the energy required to raise the temperature of an unit volume by 1 ^{0}C (or Kelvin degree).

Thermal conduction - The first term on the right hand side of the thermomechanical equation governs the transference of heat by thermal conduction in which the heat passes through the material to make the temperature uniform in the specimen. Where an unsteady state exists, the thermal behavior is governed not only by its thermal conductivity but also by its heat capacity. The ratio of these two properties is termed the thermal diffusivity $\alpha = K/C$ (m^2 s^{-1}) which becomes the governing parameter in such a state. A high value of the thermal diffusivity implies a capability for rapid and considerable changes in temperature. It is important to bear in mind that two materials may have very dissimilar thermal conductivities but, at the same time, they may have very similar diffusivities.

Thermoelasticity - The second term illustrates the thermoelastic effect. Within the elastic range and when subjected to tensile or compressive stresses, a material experiences a reversible conversion between mechanical and thermal energy causing it to change temperature. Provided adiabatic conditions are maintained, the relationship between the change in the sum of the principal stresses and the corresponding change in temperature is linear and independent of loading frequency. It is the reversible portion of the mechanical energy generated ; this thermoelastic coupling term may be significant in cases of isentropic loading.

Intrinsic dissipation - The third term is the energy dissipation generated by viscosity and/or plasticity. Internal energy dissipation was recognized by many scientists. The work done to the system by plastic deformation is identified as the major contribution to the heat effect. In thermo-elastic-plasticity, there exists a general acceptance that not all the mechanical work produced by the plastic deformation can be converted to the thermal energy in the solid. A larger portion of work is believed to have been spent in the change of material microscopic structure. The work done in plastic deformation per unit volume can be evaluated by integrating the material stress/strain curve. This internal dissipation term constitutes an important part of the nonlinear coupled thermomechanical effect. The quantitative evaluation of this intrinsic dissipation for soils or geomaterials is an extremely difficult task if infrared thermography is not used.

Heat sources - The last term shows the existence of sources or sinks of heat in the scanning field. The surface heat patterns displayed on the scanned specimen may be established either by external heating referred to in literature as "passive heating" where local differences in thermal conductivity cause variations on isothermal patterns or by internally generated heat referred to as "active heating" where isothermal patterns are established by the transformation of internal energy into heat. In the case of forced convection, if fluid at the temperature of the medium is forced rapidly past the surface of the solid, it is found experimentally that the rate of loss of heat from the surface is proportional to the surface conductance or coefficient of surface heat transfer. This fact has been used for the detection and location of heat, gas or fluid leakage through geomaterials.

INFRARED VIBROTHERMOGRAPHY

Infrared thermography has been successfully employed as an experimental method for detection of plastic deformation during crack propagation under monotonic loading of a steel plate or as a laboratory nonintrusive technique for investigating damage, fatigue, creep, and failure mechanisms. The heat dissipation evidenced here is associated with a plastic work of distortion. The infrared thermographic technique commonly utilizes a photon-effect detector in a sophisticated electronics system in order to detect radiated energy and to convert it into a detailed real-time thermal picture on a video system. Temperature differences in heat patterns as fine as 0.1 ^{0}C are discernible instantly and represented by several distinct hues.

This method is sensitive, nonintrusive, nondestructive, and noncontact, thus ideally suited for records and observations in real time of heat patterns produced by the heat transformation of energy caused by friction between grains of sheared sand. No interaction at all with the specimen is required to monitor the thermal gradient. The quantity of energy W_r emitted by infrared radiation is a function of the temperature and the emissivity of the specimen. The higher the temperature, the more important is the emitted energy. Differences of radiated energy correspond to differences of temperature, since

$$W_r = \alpha\, \theta^4\, w$$

where α denotes a constant, θ the absolute temperature and ω the emissivity.

Soils present a very low thermomechanical conversion under monotonic loading. However plastic deformation, whereby sliding between grains occurs creating permanent changes globally or locally, is one of the most efficient heat production mechanisms under cyclic conditions. Most of the energy that is required to cause such plastic deformation is dissipated as heat. Such heat generation is more easily observed when it is produced in a fixed location by reversed or alternating slidings because of vibratory reversed applied loads. These considerations define the use of vibrothermography as a nondestructive method for observing the energy-dissipating ability of granular material.

A scanning camera is used which is analogous to a television camera. It utilizes a infrared detector in a sophisticated electronics system in order to detect radiated energy and to convert it into a detailed real time thermal picture in a video system both color and monochromatic. Response times are shorter than a microsecond. Temperature differences in heat patterns as fine as 0.1 ^{0}C are discernible instantly and represented by several distinct hues.

The quantity of energy W ($W\ m^{-2}\ \mu m^{-1}$) emitted as infrared radiation is a function of the temperature and emissivity of the specimen. The higher the temperature, the more important is the emitted energy. Differences of radiated energy correspond to differences of temperature.

EXPERIMENTAL RESULTS

The thermal dissipation behaviour of a fine Stampian sand (Fontainebleau sand) is studied when subject to two types of vibratory shear loading.

Cylindrical Loading : Direct Shearing - A tubular dry sand sample, characterized by its dry unit weight $\gamma_d = 15.7\ kN.m^{-3}$, its void ratio $e = 0.72$ and its relative density $I_D = 0.62$, confined under a constant isotropic pressure of 50 kPa, is directly sheared by a concentric steel cylinder excited in an axial vibratory motion by the electrodynamic generator. In this case of sollicitation, the principal stress axes rotate during loading. At the frequency of 80 Hz and with a controlled displacement of 1 mm, the characteristic threshold is exceeded and hot colours caused by heat production by friction between siliceous grains appear as shown in the Fig. 4. The temperature increase is about 6 ^{0}C for a test duration of 20 s.

Conventional Triaxial Loading : Indirect Shearing - A cylindrical dry sand sample at the same initial density confined under a pressure of 100 kPa is subjected to a vibratory axial force, generated by a steel mass, located at the top of the specimen, and excited by an electromagnetic vibrator. When the frequency reaches 87 Hz with a controlled displacement of 1 mm at the base, the specimen (70 mm diameter, 150 mm high) is subjected to stationary stress waves and presents a striction zone where the deviatoric stress level η exceeds the characteristic threshold η_c of interlocking breakdown of the granular structure. Infrared vibrothermography demonstrates the thermal dissipation of sheared granular material (Fig. 4). Coupling mechanical and thermal energies, it characterizes the sliding mechanism of grains when the granular interlocking structure breaks down on exceeding the characteristic state. This nondestructive testing technique allows records and observations in real time of heat patterns caused by friction between grains and permits a quantitative evaluation for the growth rate of thermal dissipation.

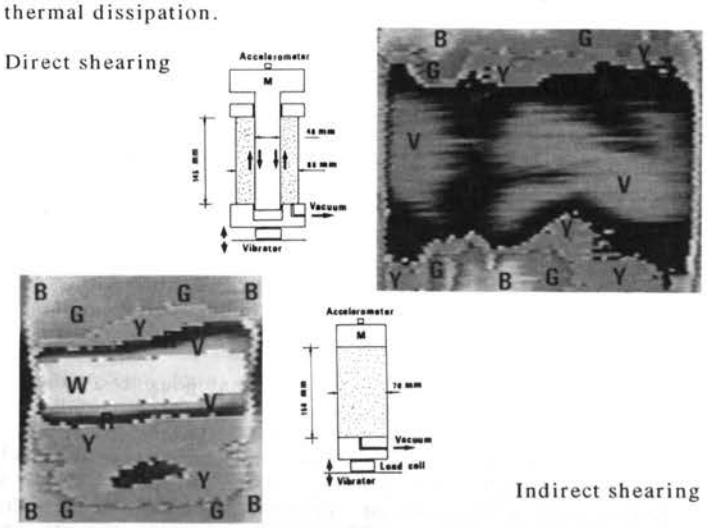

Fig. 4. Infrared thermography of the energy dissipation of a siliceous fine sand subjected to vibratory shearings (1^0 C for each color hue)

CENTRIFUGE TESTING

In dynamic geotechnical engineering, the best approach is to observe the behavior of the actual structure and check the accuracy of the existing procedure or to establish a new design technique abstracting new assumptions from observations of the full-scale structure. Unfortunately, full-scale tests to observe the behavior of an actual structure are almost always very costly, time consuming and they sometimes may be very dangerous. Furthermore, it is impossible to carry out a parametric study and to check the reproducibility of the test results. Therefore the need for scaled modeling arises to replace full-scale observations.

The scaled reproduction of wave propagation is advantageous for several reasons :
a) the problem at hand is too complex or too little explored to be amenable to an analytical solution ; empirical information on relevant physical phenomena is needed.
b) Scale models permit transformation of systems to manageable proportions and investigation of model size effects.
c) Scaled modeling shortens experimentation.
d) It promotes a deeper understanding of the phenomenon under investigation : failure mechanisms and analyses.
e) It verifies numerical models.
f) Direct modeling can be used to check the design of full scale structures.

In order to predict the prototype behavior correctly from observation, scaling laws must be established for the model and the prototype, taking into account three groups of equations governing the physical phenomena : balance equations or general laws, constitutive relations or rheological laws, and boundary conditions or initial references and boundary values. In centrifuge testing, the scaling relationship emphazises the relevant effect of self-weight induced stresses appropriate to the prototype earth structures.

EXPERIMENTAL SET-UP

The experiments were carried out in the 200g-ton centrifuge built by Latecoere in 1964 at the CEA-CESTA-centre near Bordeaux France. The arm has a radius of 10.5 m to the centre of the swinging platform. The centrifuge is equipped with 108 low noise electrical slip rings. The motor drive unit comprises 4 suspended motors (350 HP each) and 4 Ward Leonard groups (250 kVA each). The run-up time to 100g is 60 s. The rotating container of internal dimension length = 1.30 m by width = 0.80 m by height = 0.40 m, mounted on the swinging platform, was filled with Fontainebleau sand rained to the density of 1520 kgm^{-3}. The tests were run at 100g, respecting the usual scaling relationships reported in Centrifuge '88 and '91 conference proceedings (Corté 1988, Ko and McLean 1991). The motion was detected by 3D piezo-electric accelerometers which provided data on the horizontal (x), transverse (y) and vertical (z) movements at different locations in the soil mass (Fig. 5) : A1, A3, A5, A7, A9 and A2, A4, A6, A8, A10 respectively installed at 3 cm (three meters) deep and 15 cm (fifteen meters) deep. Charge amplifiers delivered a tension proportional to electric charge and independent of the capacity of the lines. All the signals were recorded on magnetic tapes. With the same magnetic tape recorders, all the signals have been read again and sent to analog channels with programmable low pass anti-aliasing filter, a hold circuit and a multiplexer. Each sample is weighted by an Hanning window. The frequency response function resolution is about 1.25 Hz. The measurement error has been evaluated at 2.5 per cent.

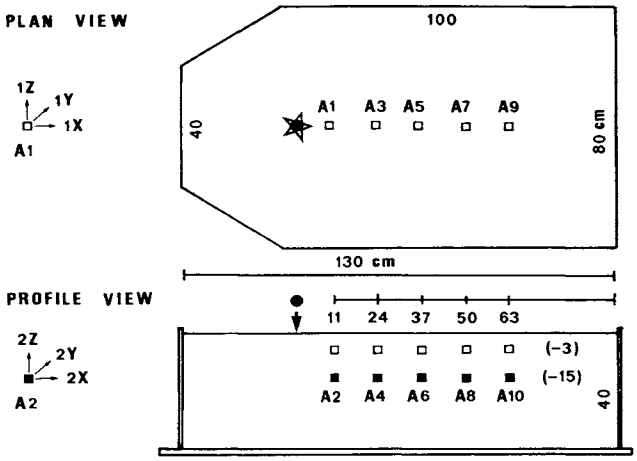

Fig. 5. Location of accelerometers in soil mass

A drop-ball arrangement (Luong 1995) has been installed in a large swinging container to produce Rayleigh shear waves. An electromagnetic motor (EMP) pushes horizontally the steel ball (SB - mass = 0.5 kg) along a guide (G) toward a thin steel wall (DC) that controls its vertical drop (DH - height = 0.1 m).

ATTENUATION WITH DISTANCE

For a vertical oscillating, uniformly distributed, circular energy source on the surface of a homogeneous, isotropic, elastic half-space, Miller and Pursey (1955) determined the distribution of total input energy among the three elastic waves to be 67 per cent Rayleigh wave, 26 per cent shear wave, and 7 per cent compression wave. The facts that two-thirds of the total input energy is transmitted away from a vertically oscillating footing by the Rayleigh wave and that the Rayleigh wave decays much more slowly with the distance than the body waves indicate that the Rayleigh wave is of primary concern for foundations on or near the surface of the earth. Because soil is not perfectly elastic, there is another consideration which influences the attenuation of R-waves. In real earth materials, energy is lost by material damping. The existence of material damping in soils is demonstrated by the fact that amplitude attenuation measured in the field is greater than would be predicted by geometric damping alone. Both geometrical and material damping is included in an expression for R-wave attenuation as follows :

$$w = w_1 \, (r_1 / r)^{-1/2} \exp [-\alpha(r - r_1)]$$

where α is the coefficient of attenuation, having dimensions of (distance)$^{-1}$. This equation implies that the total energy on two concentric circles at radii r_1 and r from a point energy source is constant except for the energy lost through material damping. Although material damping occurs in real soils, it is geometrical damping which contributes most to the attenuation of R-waves.

Thanks to the large size of the used swinging container (Fig. 5), the decrease in amplitude of the generated stress waves with depth and distance, measured by accelerometers, has been found sufficiently important to allow the assumption of negligible boundary effects.

STRESS-WAVE MITIGATION BARRIER

The dynamic response of buildings due to soil vibration can be mitigated by various different techniques :
(a) Use of friction elements at appropriate locations within a structure to increase the structural damping through energy dissipation at these locations.
(b) Change of the vibration behavior of a building by changing the soil around the foundation.
(c) Mounting of special devices such as rubber bearings, springs or a combination of springs and dampers at the foundation of the building.
(d) Reduction of the spreading waves by installing a wave barrier like a trench, a concrete wall or a wall consisting of air cushions.

The barrier disturbs the natural spreading of the waves and so screens the buildings at a certain region behind the barrier. Isolation of structures and machine foundations from ground transmitted vibrations by installation of wave barriers has been attempted many times. However this technique has met with varying degrees of success (Barkan 1962, Dolling 1966, Woods 1968, Aboudi 1973, Haupt 1977, Liao & Sangrey 1978 and Ahmad & Al-Hussaini 1991). Several numerical, experimental and analytical techniques have been applied to study the surface wave propagation across different types of barriers or in-filled trenches.

This paper presents some experimental results obtained with a new type of wave barrier, designed to dissipate seismic energy by friction between soil particles. It is suggested by a theoretical idea concerning the stability of the soil element in the presence of wave propagation. For geomaterials, experimental evidence of mechanical behavior that contradicts Drucker's stability postulate, has been shown by a great number of geotechnical researchers (Lade et al 1987, 1988).

Within the theory of plasticity, using wave propagation considerations, Mandel (1964) showed that Drucker's postulate was a sufficient but not a necessary condition for a material to be stable, due to the frictional nature of sliding between soil particles (Hardin 1978). Based on the assumption that a stable material is able to propagate a small perturbation in the form of waves, Mandel (1964) proposed a necessary condition for stability. He showed that a wave can propagate in a material with an elastic-plastic matrix **A**, along the direction α, if and only if all the eigenvalues λ of the matrix **M** are positive.

$$d\epsilon_{ij} = \mathbf{A}_{ijkl} \cdot d\sigma_{kl}$$

$$\mathbf{M}_{ik} = \mathbf{A}_{ijkl} \cdot \alpha_j \cdot \alpha_l$$

where $k = 1, 2, 3$ and $\lambda_k > 0$.

If one of the eigenvalues λ is ≤ 0, one of the corresponding components of the perturbation cannot propagate. This implies instability, and the possible appearance of strain localisation along a shear band or sliding zone along a certain direction. This phenomenon occurs when the stress state reaches the supercharacteristic domain where the frictional mechanism is very active between soil particles, or when the loading is cycled near the characteristic threshold. A very important amount of mechanical energy (several tens of kJ.m^{-3}) can then be dissipated in soil mass by heat as evidenced by infrared vibrothermography (Luong 1986).

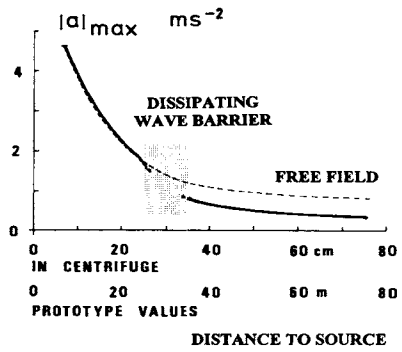

Fig. 8. Efficiency of the proposed dissipating wave barrier

In the centrifuge, a dissipating wave barrier has been simulated by applying on the soil mass additional loadings such that the stress state locally reaches the supercharacteristic threshold. This loaded region will mitigate the wave energy as shown by the decreased amplitude of acceleration records (Fig. 8). Centrifuge results reveal to be very promising. However these results must be validated by field tests.

CONCLUSION

Centrifuge simulation of wave propagation in soils is very useful for a realistic evaluation of the dynamic soil properties involved in the interpretation of the geotechnical performance of earthquake-resistant and vibration-isolating structure models.
This technique provides a reliable representation of : (1) soil modulus varying with depth, (2) frequency variability of the soils resulting from soil inertia, damping reactions caused by elastic wave radiation and internal friction and (3) both kinematic and inertial soil-structure interactions. It aims to elucidate the relevant parameters influencing the rheological behavior of geotechnical structures subjected to transient and dynamic loadings.
The proposed technique of in flight falling-weight source offers a very simple means of applying a substantial transient force normal to the ground surface during the impact.
Artificially generated seismic waves provide useful information about the mechanical characteristics of soil in flight, facilitating the analysis of dynamic centrifuge test results. Such centrifuge model experiments offer promise for future application on seismic or vibratory isolation of geotechnical structures.

REFERENCES

Aboudi, J. (1973), "Elastic waves in half-space with thin barrier", J. Engng Mech. Div., ASCE, 99(1): 69-83.

Ahmad, S. and T.M. Al-Hussaini (1991), "Simplified design for vibration screening by open and filled trenches", J. Geot. Engng, ASCE, 117(1): 67-88.

Barkan, D.D. (1962), "Dynamics of basis and foundations", Mc Graw Hill, New York.

Bowden, F.P. & D. Tabor (1959), "Friction and lubrification", Monographies, Dunod, Paris.

Corté, J.F. ed. (1988), "Centrifuge '88", Rotterdam: Balkema.

Dillon, O.W.Jr (1963), "Coupled thermoplasticity", J. Mech. Phys. Solids, 11: 21-23.

Dolling, H.J. (1966), "Efficiency of trenches in isolating structures against vibrations", Proc. Symp. Vibration in Civil Engineering, Butterworths, London, 273-276.

Hardin, B.O. (1978), "The nature of stress-strain behavior of soils", Proc. Conf. Earthquake Engineering and Soil Dynamics, ASCE, Pasadena, USA, 1: 3-90.

Haupt, W.A. (1977), "Isolation of vibration by concrete core walls", Proc. 9th ICSMFE, JSMFE, Tokyo, 2: 251-256.

Hoar, R.J. and K.H. Stokoe (1984), "Field and laboratory measurements of material damping of soil in shear", Proc. 8th World Conf. Earthquake Engng, San Francisco, III: 47-54.

Ko, H.Y. and F.G. McLean ed. (1991), "Centrifuge 91", Rotterdam: Balkema.

Kratochvil, J. and O.W. Dillon (1969), "Thermodynamics of elastic-plastic materials as a theory with internal state variables", J. Appl. Phys., 40: 3207-3218.

Lade, P.V., Nelson, R.B. and Y.M. Ito (1987), "Nonassociated flow and stability of granular materials", J. Engng Mech., ASCE, 113(9): 1302-1318.

Lade, P.V., Nelson, R.B. and Y.M. Ito (1988), "Instability of granular materials with nonassociated flow", J. Engng Mech., ASCE, 114(12): 2173-2191.

Liao, S. and D.A. Sangrey (1978), "Use of piles as isolation barriers", J. Geot. Engng Div., ASCE, 104(9): 1139-1152.

Luong, M.P. (1980), "Stress-strain aspects of cohesionless soils under cyclic and transient loading", Proc. Int. Symp. on Soil under Cyclic and Transient Loading, Rotterdam: Balkema, 315-324.

Luong, M.P. (1986), "Characteristic threshold and infrared vibrothermography of sand", Geotechnical Testing J., GTJODJ, 9(2): 80-86.

Luong, M.P. (1992), "Energy-dissipating ability of sandy soils", Proc. 10th World Conf. Earthquake Engineering, Balkema 1992, 3: 1209-1214.

Luong, M.P. (1995), "Centrifuge simulation of Rayleigh waves in soils using a drop-ball arrangement", Dynamic Geotechnical Testing II, ASTM STP 1213, Ebelhar, Drnevich and Kutter eds.

Mandel, J. (1964), "Conditions de stabilité et postulat de Drucker", Proc. IUTAM Symp. Rheology and Soil Mechanics, Grenoble, 58-68.

Miller, G.F. and H. Pursey (1955), "On the partition of energy between elastic waves in a semi-infinite solid", Proc. Royal Society, London, A, 233, 55-69.

Mindlin, R.D. and H. Deresiewicz (1953), "Elastic spheres in contact under varying oblique forces", J. Appl. Mech., 20, 327-344.

Mok, Y.J., I. Sanchez-Salinero, K.H. Stokoe and J.M. Roesset (1988), "In situ damping measurements by cross-hole seismic method", Proc. Earthquake Engng and Soil Dynamics, ASCE Spec. Conf., Utah, 305-320.

Ray, R.P. and R.D. Woods (1988), "Modulus and damping due to uniform and variable cyclic loading", J. Geotech. Engng, ASCE, 114(8): 861-876

Stewart, W.P. and R.G. Campanella (1991), "In situ measurement of damping of soils", Proc. 2nd Int. Conf. Recent Advances Geotech. Earthquake Engng Soil Dynamics, March 11-15, 1991, St Louis, I: 83-92.

Teachavorasinskun, S., S. Shibuya, F. Tatsuoka, H. Kato and N. Hori (1991), "Stiffness and damping of sands in torsion shear", Proc. 2nd Int. Conf. Recent Advances Geotech. Earthquake Engng Soil Dynamics, March 11-15, 1991, St Louis, I: 103-110.

Tonouchi, K., T. Sakayama and T. Imai (1983), "S-wave velocity and the damping factor", Bull. Int. Assoc. Eng. Geol., Paris, 26-27: 327-333.

Woods, R.D. (1968), "Screening of surface waves in soils", J. Soil Mechanics and Foundations Div., ASCE, 94(SM4): 951-979.